Research Article
Volume 14: 01, 2025

Molecular Biology: Open Access

ISSN: 2168-9547 Open Access

Activated Carbon (AC) Derived from Pre-carbonized Date Palm Leaves (PCDPLs) Activated with Lithium Chloride (LiCl): Physical and Electrical Properties

Fatima Musbah Abbas[1*], Ahlam Khalofa[2], Abubaker Elsheikh Abdelrahman[3] and Selma Elsheikh Abdelrahman[4]

[1]*King Khalid University, Collage Science and Art, Dhahran Aljanoub, Abha, Saudi Arabia*

[2]*Department of Biology, King Khalid University, Abha, Saudi Arabia*

[3]*College of Science, Hafralbatin University, Hafralbatin, Saudi Arabia*

[4]*Act Center for Research, Singa, Sudan*

Abstract

Activated Carbon (AC) is a porous material widely utilized in energy storage, electromagnetic wave absorption and, among many other applications. Despite the economic and environmental benefits of recycling date palm leaves (*Phoenix dactylifera L.*) into AC, there is limited research on the characterization of AC produced *via* date palm leaves, particularly in pellet form. The study aims to evaluate the structure, mechanical and electrical properties of "Activated Carbon Pellets (ACPs)" derived from "Pre-Carbonized Date Palm Leaves (PCDPLs)" with varying concentrations of LiCl. The ACPs were ball-milled, treated with LiCl and pelletized before undergoing carbonization at 700 ℃. The resulting Activated Carbon Pellets (ACPs) were analyzed for particle size distribution, bulk density, Young's Modulus (YM), crystallite dimension, Specific Surface Area (SSA) and Electrical Conductivity (EC). The percolation theory was applied to analyze YM data. Results indicated that YM increased with LiCl concentration, with the highest value observed at 1.2 M LiCl. The critical density for YM, determined using percolation theory, was 0.7 g/cm^3. The ACPs exhibited SSA ranging from 1099.1 to 1545.8 m^2/g and the EC varied from 0.531 and 0.642 × 10^5 (Ohm'm)$^{-1}$, demonstrating a significant enhancement compared to untreated samples. In conclusion, LiCl activation, combined with controlled heating, significantly improves the physical and electrical properties of ACPs made from date palm leaves, with bulk density being a key factor in these improvements.

Keywords: Activated carbon pellets • Date palm leaves • LiCl activation • Young's modulus • XRD • Specific surface area • Electrical conductivity • Young's modulus • Percolation theory • Pellet form

Introduction

"Activated Carbon (AC)" is a type of absorbent substance widely manufactured in research laboratories. In addition to being an active component in double-layer capacitors [1,2], it is utilized for several other purposes, such as energy storage [3], effective electromagnetic wave absorption [4], water purification [5], greenhouse gas adsorption [6] toxic substance removal [7] and the uptake and removal of methylene blue [8]. The adsorptive capabilities of AC are attributed to its unique characteristics, which are utilized in a variety of liquid and gas phase applications [9].

AC can be prepared from carbonaceous materials by either a chemical or physical method. The chemical method involved an activation process with the suitable chemical agent in order to improve the pore-sized distribution on the surface, facilitating absorption capacity. Therefore, several carbon-rich substances have been examined to create AC with a large surface area, such as oil palm leaves [10] oil palm empty fruit bunches [11,12] olive stone [13] cellulose material [14] coconut shell [15] soybean dregs [16] and date palm leaves [17].

Furthermore, AC materials are usually synthesized as pellets, granules and powders. The pellet form is dense, chemically stable and uniform with fewer voids, which makes the characterization of physical, electrical properties and surface morphology easier. Electromechanical applications of carbon materials require excellent chemical stability, homogeneity, density and adequate contact points. Hence, measuring electrical and physical conductivity is essential. Consequently, multiple methods have been utilized to improve the characteristics of AC substances such as the pyrolysis mechanism [18,19] pelletizing pressure [15,20] and activation process [15,21,22].

The present study addresses the challenge of manufacturing AC *via* renewable resources with benefits including low cost, low ash and high carbon content. Date Palm Leaves (DPL) have been recognized as a promising precursor. Despite the possible economic benefits of recycling palm leaves into useful products as highlighted [23]. The Date Palm Leave (DPL) is classified as lignocellulose biomass, which is typically composed of cellulose, hemicellulose and lignin as the main products and the pyrolysis mechanism are reported elsewhere [24]. There is extensive research on chemical activation by KOH [15,25,26], K_2CO_4 [21,22] and H_3PO_4 [22,27] but is not much research on the detailed characterization of AC made from date palm leaves chemically activated with LiCl especially in the pellet form. The LiCl compound has been used in medical applications as well as the identification of mood-stabilized regulators [28], as bipolar disorder treatment [29] and as promoting the proliferation of neural stem cells [30]. Also, the physical properties of LiCl have been studied elsewhere [31]. Moreover, the structural, mechanical and electrical characteristics of AC as a function of activating agent concentration have not been extensively examined in prior research. This research aims to fill this gap by evaluating the structure, crystallite dimension, bulk density, Young's modulus, specific surface area and Electrical Conductivity (EC) of AC pellets made from DPL. The study utilizes a multistep heating profile to activate with LiCl and carbonized at 700 ℃ in a nitrogen environment in order to determine the Young's modulus and determine the critical density at which Young's modulus disappears by applying the percolation theory is subsequently applied to analyse the results. Moreover, the crystallite dimensions, correlation between crystallite dimensions and specific surface area and bulk density and, finally, electrical conductivity were investigated and the results were compared with data that had been previously published.

***Address for Correspondence:** Fatima Musbah Abbas, CKing Khalid University, Collage Science and Art, Dhahran Aljanoub, Abha, Saudi Arabia; E-mail: fatima_musbah09@outlook.com*

***Copyright:** © 2025 Abbas FM, et al. This is an open-access article distributed under the terms of the Creative Commons Attribution License, which permits unrestricted use, distribution and reproduction in any medium, provided the original author and source are credited.*

Received: 03 February, 2025, Manuscript No. MBL-25-162517; **Editor Assigned:** 05 February, 2025, PreQC No. P-162517; **Reviewed:** 17 February, 2025, QC No. Q-162517; **Revised:** 24 February, 2025, Manuscript No. R-162517; **Published:** 04 March, 2025, DOI: 10.37421/2168-9547.2025.14.472

Methodology

Sample preparation

The date palm leaves were first allowed to air dry for three weeks, then were crushed into smaller fragments. These fragments exhibited microstructural disturbance, shrinkage and weight loss after a 4-hour pre-carbonization process. According to Abbas FM, et al. [32] the emission of volatile components and tar was the primary cause of the mean weight loss of nearly 31%. To improve their self-adhesive characteristics, the PCDPLs underwent ball milling for 20 hours to achieve a finely ground powder. The result of the particle size distribution of the fine grain powder is illustrated in Figure 1. The fine grain powder was then treated with different concentrations of LiCl (0-1.6) by Moles (M) in a separate glass container. After 16 hours of magnetic stirring, each mixture was dried for 4 hours at 100℃. After milling the dried mixture for 5 more hours, it was then sieved. In accordance with the method provided by Abdulrahman AE, et al. [15] utilizing a "Vulcan Box Furnace 3-1750", two grams of PCPLs were pelletized under a pressure of 15 metric tons prior to carbonization "at 700℃ in a nitrogen atmosphere utilizing a multistep heating profile". Subsequently, the system was allowed to gradually cool to room temperature. The carbon pellets were then thoroughly cleaned with hot distilled water to remove LiCl particles and impurities until a pH of 6 was reached. Results were averaged from five replicates of each sample and analyzed based on the LiCl (M). A micrometer was utilized to measure the pellet's dimensions both before and after carbonization and the bulk density was measured.

"Young's Modulus (YM)" of carbon pellets was measured utilizing "ultrasonic techniques". The signal from the Ultrasonic pulsar receiver (Model 500 PR) was analyzed by PICO ADC 200 software for the calculation of longitudinal ultrasonic Velocity (v) and YM in the sample. The ultrasonic signal was standardized utilizing (Sigradur-K), a standard glassy carbon material. The one-dimensional form of the wave Equation is represented by YM as follows.

$$YM = \rho V^2 \quad (1)$$

A threshold from percolation theory above the critical density (ρ_c) was utilized to examine the findings of YM data as [33].

$$YM \sim (\rho - \rho_c)^t \quad (2)$$

Where ρ_c is the critical density,

Plotting logarithm YM against logarithm (ρ-ρ_c) (Equation 3) for densities (ρ) higher than ρ_c for many values of ρ_c always results in a linear relationship with slope (t) equal to 2 [34]

$$\log YM \sim (\rho - \rho_c) \quad (3)$$

Utilizing "Bruker Advanced Solution AXS D8 equipment working at 40 kV and 30 mA", the "X-ray Diffraction (XRD)" profiles of "Activated Carbon Pellets (ACPs)" were produced. The "Cu Kα X-ray radiation" applied had a wavelength (λ) of 1.5406 Å. "Pellets were scanned at 2θ angles with a step size of 0.04°", encompassing a range of 10° to 80°. Corrections were made for instrumental broadening and background line intensity in the XRD data. Graphitic-like crystallite stacking height (L_c) was calculated with the "Trace 1.4 program from Diffraction Technology" by applying Bragg's Equation and Sherrier Equation. This program removes Kα2 peaks from diffraction patterns, smooths peak shape, subtracts background lines and adjusts individual peak intensities [17].

$$L_{c,a} = \frac{k\lambda}{\beta_{c,a}\cos\theta} \quad (4)$$

Where "θ is the scattering angle position, l is the wavelength of X-ray diffraction, K is a shape factor which is equal to 0.9 for Lc and 1.84 for La and β c,a is the width of a reflection at half- height expressed in radians".

The relationships between $d00_2$ and L_c can be deduced by assuming that for large L_c=1/L_c approaches zero, then $d00_2$ *vs.* 1/L_c should follow a linear relation as [15],

$$d_{002} = 3.354 + \frac{\varphi}{L_c} \quad (5)$$

Where 3.354 is the $d00_2$ for the pure graphite structure and φ is the slope.

The amorphous content was estimated by the Richards BP [35] assumption as the interlayer spacing could be related to the probability that the nearest neighbor layer planes are ordered (p_1) for turbostratic carbon by the following equation

$$d_{002} = 0.3351 + 0.086(1 - p1) \quad (6)$$

Total probability=probability that the nearest neighbor ordered (crystal content) (P_1) + probability that the nearest neighbor are disordered (amorphous content) (P_2) =1 then the amorphous content (p_2) can be given as:

$$p_2 = 1 - p_1 \quad (7)$$

The Equation 6 given written as

$$d_{002} = 0.0334 + 0.086\,p2 \quad (8)$$

The values of amorphous content was calculated manually as the following Equation:

$$p2 = \frac{(d_{002} = 0.3354)}{(0.086)} \times 100$$

The "Surface Area (SA)" of porous material can be estimated from the Bulkdensity (ρ) and Stack Height (L_c) of the graphitic-like structure have been proposed by Dresselhaus MS, et al. [36] and further used by the Arof AK, et al. [37] and Abdulrahman AE, et al. [15].

$$S = \left(\frac{2}{\rho L_c}\right) \quad (9)$$

DC " Electrical Conductivity (EC)" was measured *via* " four-point-probe equipment (Keithley Micro-Ohmmeter)" as:

$$EC = R\frac{d}{A} \quad (10)$$

Where "d is the sample thickness, R (Ohm) is the electric resistance and A is the area of the sample". The accuracy of the data was subsequently verified *via* a graphite sheet as a reference standard.

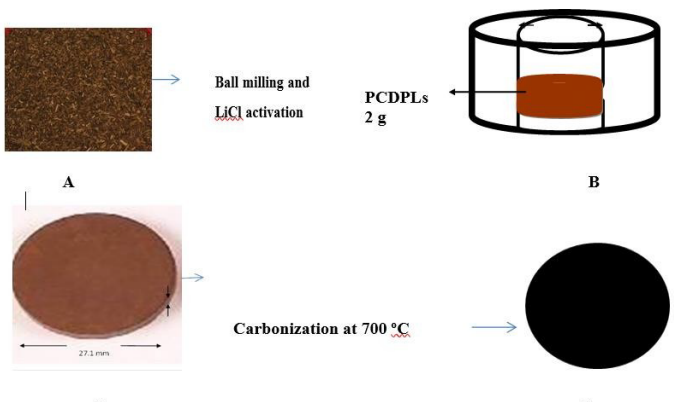

Figure 1. **A)** Raw PCDPLs, **B)** Palletization mold, **C)** PCDPLs pellets and **D)** ACP produced at 700 ℃.

Results and Discussion

Particle size distribution of the PCDPLs

The particle size distribution of PCDPLs produced by the ball milling process for 20 hours is illustrated in Figure 2. The Figure exhibits a strong positive correlation between LiCl and YM, indicating that as the value of LiCl increases, so does the value of YM. The samples displayed different distributions, skewed towards the larger sizes of the following distribution: 6 percent ›100 µm, 10 percent 43–50 µm, 40 percent ‹26.2 µm and 14 percent >16.3 µm Figure 4 showing most of the particle sizes were ‹50 µm.

Bulk density and Young's modulus

Table 1, shows the results of bulk density measurements, ranging from 1.348 to 1.380 g/cm^{-3}. The bulk densities of the ACPs increased rapidly from 0 to 1.2M LiCl and then decreased thereafter. This suggests that a concentration of 1.2M LiCl yields the highest bulk density as compared to the other concentrations, which is significant for producing densely activated carbon pellets. The results determined that an increase in ρ values is accompanied by an increase in longitudinal (V), which contributes to changes in the YM of the ACPs produced.

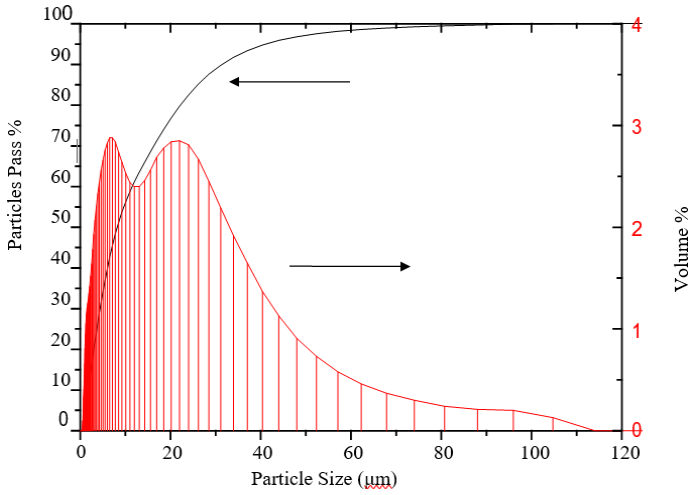

Figure 2. Particle size distribution of the PCDFLs milled for 20 hrs.

Table 1 and Figure 3 determined that the YM of the ACPs increased minimally from "5.8 GPa to 10.7 GPa", aligning with the YM of ACPs from the date palm leaves treated with KOH (5.35- 10.53) GPa as reported by Abdulrahman AE, et al. [15]. Additionally, the YM range for solid carbon pellets from DPL, prepared at various compression pressures(5 GPa-7.1 GPa), suggests that both KOH treatment and compression pressure have comparable effects [20]. This observation is consistent with our findings on the response of KOH concentration, suggesting a similar response to compression pressure. The highest YM value of 10.53 GPa was observed at a KOH concentration of 0.25M, exhibiting that LiCl activation increases the mechanical performance of the grain powder and optimizes the activation process for palm leaf grain powders.

Percolation theory

Additionally, YM, as per percolation theory, was analyzed for ACPs with densities exceeding the critical density ($\rho > \rho_c$) by fitting Log YM *vs.* Log ($\rho-\rho_c$) as illustrated in Figure 4 and represented by Equation (2). The fitting process involved altering the values of ρc until achieving the best linear curve fit, resulting in a slope of 2.12, which is very close to the accepted universal value of t=2 [34]. "The y-axis intercept is -4.9 and the fitting value of ρc was revealed to be 0.7 g/cm^3", representing the percolation threshold or critical density before YM disappears. "This indicates that the percolation theory correlates with the bulk density of the carbon samples as interpreted by the increase in the bulk density of the sample above 0.7 g/cm^3. This value is higher than the critical density of the activated carbon base treated with KOH of (0.05 g/cm^3) [38] and is almost three times than that for solid carbon pellets derived from DPL treated with a different compression pressure (0.025 g/cm^3) [34]. These results confirm the validity of percolation theory in describing how YM variations for ACPs depend on LiCl treatment in relation to percolation transition.

Figure 4 illustrates a scatter plot exhibiting a positive relationship among pressure difference log(p-p_c) and Log(YM) indicating that as the Log(p-p_c) value increases, the Log(YM) value also tends to increase. Thus, it can be concluded that YM of the material increases with increasing pressure difference.

Table 1. LiCl (M), Bulk Density (ρ), Longitudinal Velocity (V), YM (GPa), Log (YM) and Log (p- pc) of ACPs produced.

LiCl (M)	ρ (g/cm^{-3})	V (m/s)	YM (GPa)	Log (YM)	Log (p-pc)
0	1187 ± 26.12	2216.58	5.832 ± 0.124	0.766	2.688
0.2	1230 ± 31.01	2385.4	6.999 ± 0.082	0.845	2.724
0.4	1264 ± 23.91	2499.49	7.897 ± 0.562	0.897	2.751
0.6	1301 ± 22.85	2548.61	8.451 ± 0.411	0.927	2.779
0.8	1318 ± 19.32	2692.11	9.552 ± 0.501	0.980	2.791
1	1325 ± 21.09	2764.48	10.126 ± 0.43	1.005	2.796
1.2	1358 ± 25.67	2804.78	10.683 ± 0.62	1.029	2.818
1.4	1314 ± 20.87	2772.59	10.101 ± 0.452.	1.004	2.788
1.6	1296 ± 26.33	2736.18	9.703 ± 0.337	0.987	2.775
Abbas FM, et al. [17]	-	-	7.03-10.15	-	-
Abbas FM, et al. [20]	-	-	2.81-6.92	-	-
Sigradur-K (from the suppliers	1540	-	35.70	-	-
Sigradur-K	1540	-	34.90	-	-

XRD

The XRD analysis found that the structure of all the carbon pellets produced is a turbostratic carbon structure, due to the presence of a considerable quantity of amorphous carbon in the sample, as revealed by the higher background line in the X-ray diffraction intensity profiles as shown in Figure 5. This Figure illustrates a black curve labeled raw X-ray data exhibiting the intensity of the X-rays diffracted by the sample before any corrections were made. It also displays a red curve labeled X-ray data corrected to the background line exhibiting the intensity of the diffracted X-rays after subtracting the background signal. This correction has been applied, revealing "two broad diffraction peaks corresponding to (002) and (100) reflection"

Planes located at approximately 23.55-24.2° and 43.59-44.9° diffraction angles (Two θ), respectively. The corrected X-ray diffraction data was further fitted in Gaussian distribution carve to release interference data as displayed in Figure 6. Finally, Figure 7 represent the trace X-ray programs used to calculate the crystallite dimensions (L_c and $d00_2$).

The crystallite dimension (L_c) values were calculated using Equation (1) with trace X-ray diffraction programs to assess measurement accuracy as

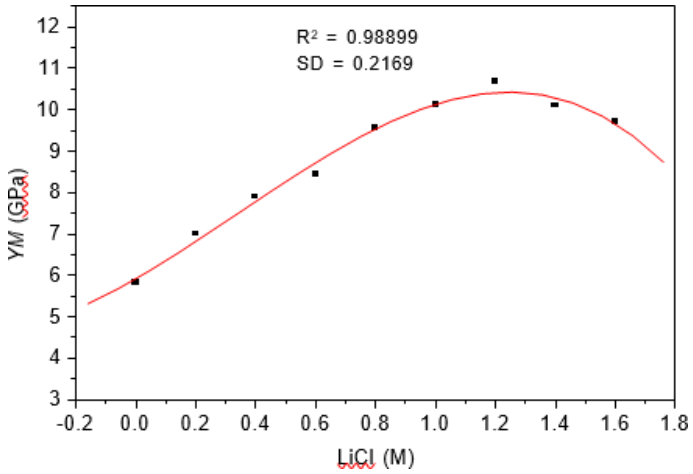

Figure 3. YM *vs.* LiCl (M).

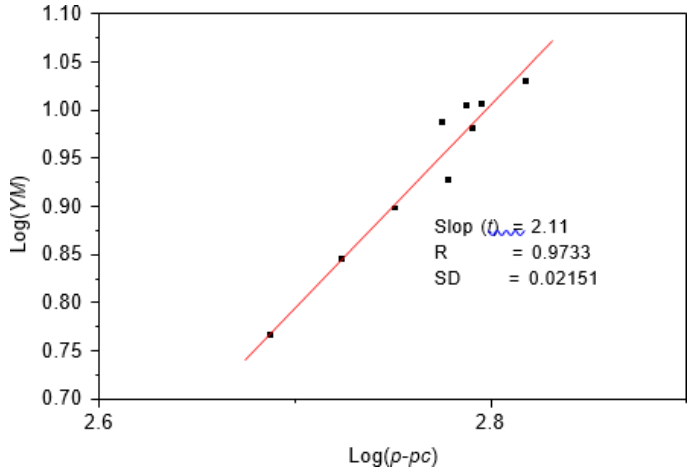

Figure 4. Log (YM) *vs.* Log (ρ-ρc) to estimate critical density (ρc).

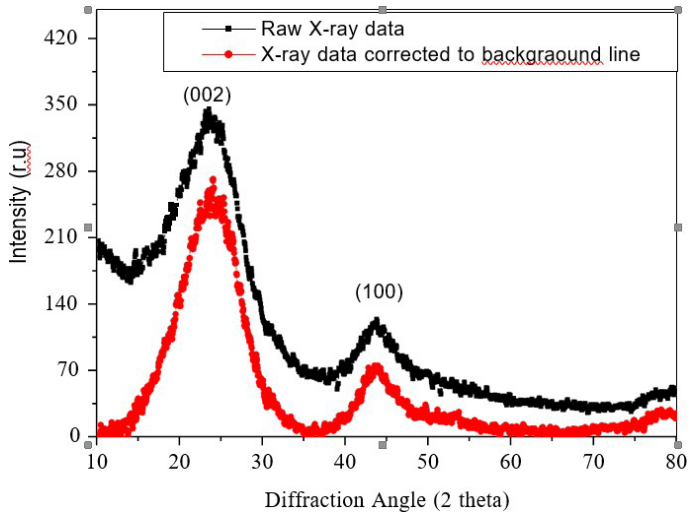

Figure 5. XDR data of the ACP raw data and corrected data background line to zero intensity profiles.

provided in Table 2 and Figure 8. The L_c values range from almost 0.88 nm to 1.34 nm, corresponding to approximately~ 3 to 4 graphene layers with an interlayer spacing equal to that of a pure graphite structure (approximately ~3.35 Å) and the interlayer spacing, $d00_2$ values range from 0.3596 nm to 0.3633 nm, as represented in Table 2 and Figure 6. The Lc values produced are comparable to those of ACPs from date palm leaves treated with KOH (0.99 nm-1.08 nm) [34]. This values is lower that solid carbon in pellets form based on date palm treated with different compression pressure, the L_c values in the

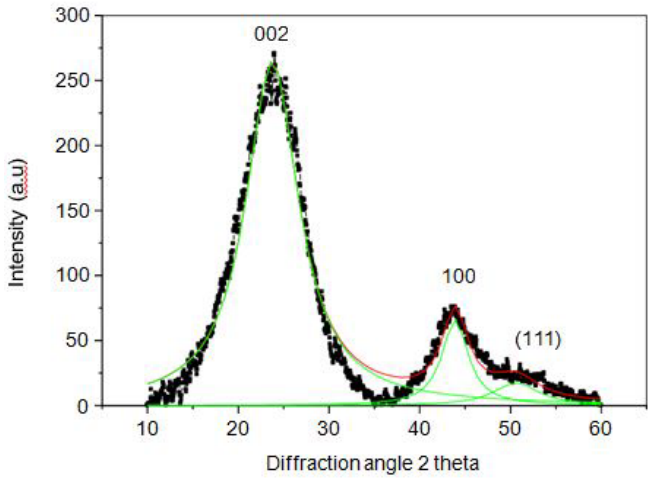

Figure 6. XDR data of the ACP corrected data fitted into Gaussian curve.

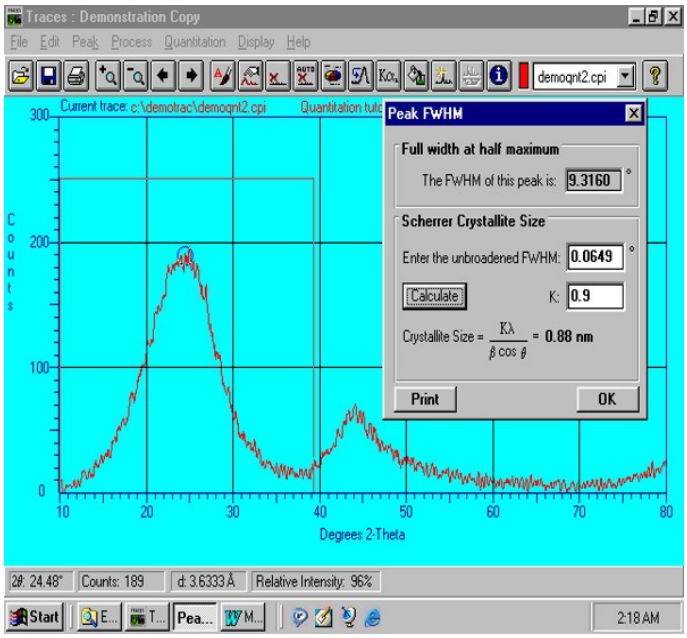

Figure 7. Trace, XRD program used to calculate crystallite dimension.

range from 1.56 nm-1.82nm with $d00_2$ values similar to that of activated carbon type H (Ac-TypH (0.36 nm) [39]. The staking order or crystallite dimension (L_c) of the ACPs varied with bulk density, indicating that the improvement in staking orders depends on bulk density, as illustrated in Figure 8. In addition, the relationship between $d00_2$ and L_c was found to obey the linear Equation of $d00_2$ *vs.* 1/ L_c,

Where $d00_2$ approaches 0.3354 where L_c approaches infinity and the slope (φ) is equal to=0.00822 $(nm)^2$ as shown in Figure 8 and the Equation (8) is given as:

$$d_{002} = 0.3354 + \frac{0.00822}{L_c} \quad (11)$$

Constant φ=4.13 and the cut y- axis equal to 3.366 Å which is close to that of purr graphite 3.354 Å, given by Equation (2), justifying that the crystallite dimensions can be controlled by stacking height of the non-gradation composite carbon material.

The measurements of the amorphous content give pc values in a range 0.3244–0.28256 indicating the structure of the carbon sample to be about 32.44 to 28.256 % amorphous structure as summarized in Table 2 and plotted in Figure 9. These findings indicate that the LiCl applied on pre-carbonized

Table 2. LiCl (M), Stack height (L_c), and interlayer spacing ($d00_2$) and p_2 % of ACPs produced.

LiCl (M)	L_c (nm)	d_{002} (nm)	Amorphous Content (p_2) %
0.0	0.88 ± 0.42	0.3633	32.44
0.2	1.16 ± 0.33	0.3622	31.163
0.4	1.22 ± 0.09	0.3619	30.814
0.6	1.24 ± 0.11	0.3605	29.186
0.8	1.26 ± 0.08	0.3601	28.721
1.0	1.28 ± 0.06	0.3598	28.372
1.2	1.34 ± 0.61	0.3597	28.256
1.4	1.31 ± 0.52	0.3596	28.1410
1.6	1.28 ± 0.43	0.3605	29.186
Faber K, et al. [39]	0.7	0.360	-
Abbas FM, et al. [20]	1.56-1.82	0.365-0.370	-
Abbas FM, et al. [32]	9.2-13.5	-	-
Azahar AA, et al. [38]	8.4-13.5	-	-

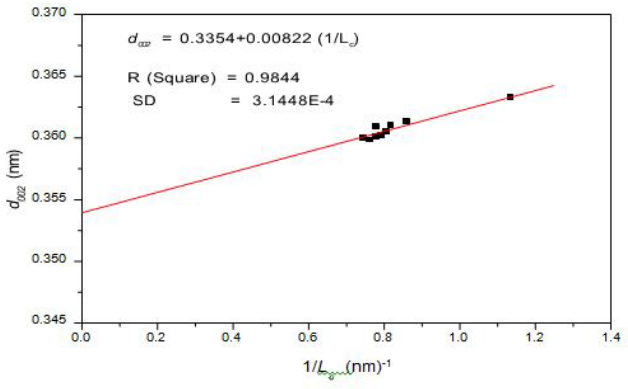

Figure 8. d_{002} *vs.* $1/L_c$.

date palm leaves powder can transform the crystalline carbon structure to a more crystallite state.

Specific Surface Area (SSA)

The SSA of carbon produced was calculated using Equation (2) as represented in Table 2 and Figure 10, exhibiting that LiCl activation can produce carbon pellets with high specific surface areas ranging from 1099.1–1545.8 m^2/g, characterized by an acceptable pore structure. This finding aligns with the non-permeable carbon derived from oil palm leaves treated with KOH, which exhibit an SSA of 1658 m^2/g [32] and higher than those from olive stones activated with H_3PO_4, 1221 m^2/g) Yakout SM and El-Deen GS [27]. From activated carbon monoliths and carbon nanotube [40] and oil palm empty fruit bench 1215 m^2/g [41,42]. Notably, the untreated sample with LiCl (0 M) exhibits the highest specific surface area among the ACPs, indicating the prevalence of microporous, mesoporous structure compared to other samples. This suggests that LiCl activation can manufacture CPs with highly specific surfaces suitable for various applications, including increased adsorption properties and as electrodes for supercapacitors. These results highlight the beneficial impact of LiCl activation on improving the SSA of the produced AC (Table 3).

Electrical Conductivity (EC)

Table 2 represents the electrical conductivity of the ACPs produced, plotted against LiCl (M) in Figure 11. The results revealed that 1.2 M LiCl exhibited higher EC as compared to other concentrations attributed to increased electrical contacts between conducting microcrystalline. This indicates that the samples benefited from enhanced conductivity through LiCl activation due to improved formation of conductive layers. Furthermore, carbon with a higher EC generally suggests a more ordered structure as compared to lower EC samples. The relationship between EC and bulk density is illustrated in Figure 10, exhibiting a linear relationship where the EC of the ACPs varies with bulk density. This indicates that the increment of the EC depends on the bulk density of the ACPs or the products produced as depicted in Figure 12.

Conclusion

The Activated Carbon Pellets (ACPs) were successfully prepared employing LiCl activations. The YM of these ACPs was consistent with those

Table 3. LiCl (M), Specific Surface Area (SSA) and Electrical Conductivity (EC).

LiCl (M)	SSA (m^2/g)	EC x10^5 (Ohm-m)$^{-1}$
0.0	1545.8 ± 47.3	0.531 ± 0.005
0.2	1401.7 ± 51.2	0.558 ± 0.01
0.4	1297.0 ± 44.1	0.580 ± 0.007
0.6	1239.7 ± 37.5	0.604 ± 0.007
0.8	1204.3 ± 38.4	0.615 ± 0.006
1.0	1179.3 ± 51.2	0.620 ± 0.011
1.2	1099.1 ± 49.6	0.642 ± 0.008
1.4	1161.9 ± 55.1	0.613 ± 0.012
1.6	1205.6 ± 46.2	0.601 ± 0.006
Abbas FM, et al. [32]	1308-1658	-
Dolah BNM, et al. [40]	987-1704	-
Yakout SM and El-Deen GS [27]	1221	-
Yulianti RT, et al. [41]	1225	-
Graphite	-	~1×10^5

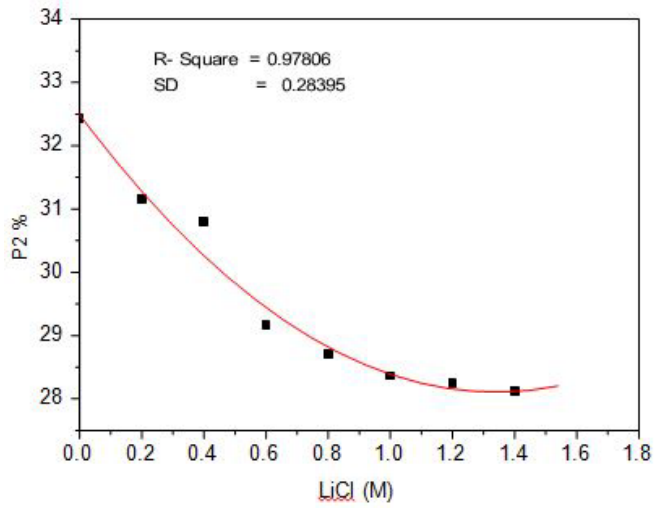

Figure 9. P_2% *vs.* LiCl (M).

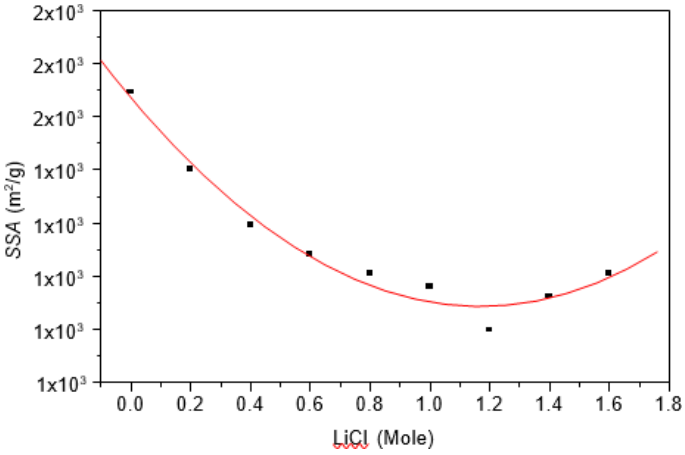

Figure 10. SSA *vs.* LiCl (M).

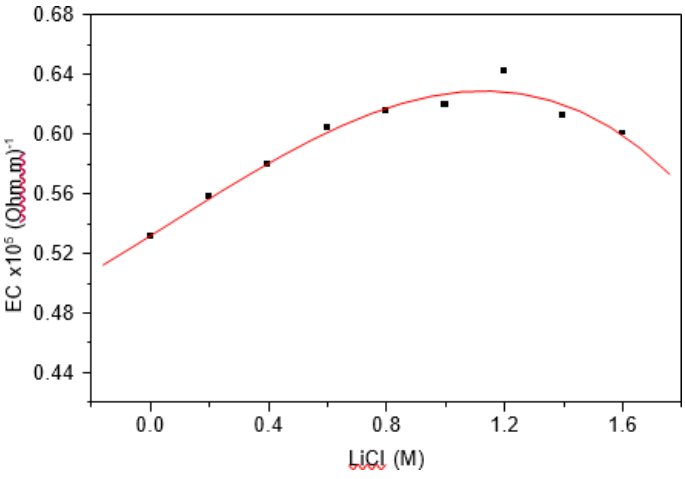

Figure 11. EC *vs.* LiCl (M).

prepared from pre-carbonized samples activated with KOH. Percolation theory demonstrated a significant correlation with the bulk density of the carbon samples, indicated by the "increase in bulk density of the AC sample above the critical density of 0.7 g/cm³ for YM". The structure of all the carbon pellets produced is a turbostratic, with crystallite dimensions improved by increasing the LiCl concentrations up to 1.2 M. in addition, the LiCl (M) activation caused to transform the crystalline structure of the AC produced to a more crystallite state.

The specific surface area of the ACPs ranges from 1099.1–1545.8 m²/g, making them suitable for numerous applications. The EC of ACPs was found

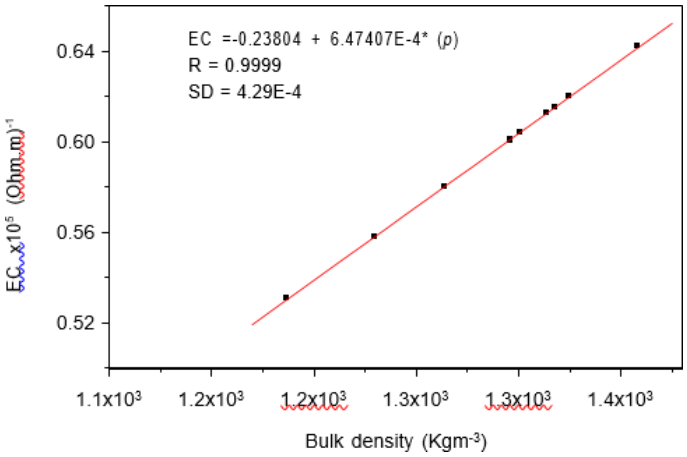

Figure 12. EC as a function of bulk density.

in the range of 0.531-0.642 × 10^5 (Ohm'm)$^{-1}$, more than half the value of pure-graphite (~1 × 10^5), indicating significant improvement through LiCl activation. Therefore, the combination of LiCl activation and a heating profile of up to 700 ℃ and pre-carbonized properties of DPL play an essential role in enhancing the physical and electrical properties of the produced ACPs. The bulk density of ACPs varied linearly with their EC, indicating that the improvement is dependent on bulk density.

Limitation and Future Implications

The study limitations include a limited temperature range (700 ℃) and reliance on a single LiCl activation method. Additionally, the study was restricted to date palm leaves as the precursor, which may not be generalized to other carbonaceous materials. In order to further improve the electrical and physical characteristics of ACPs, future studies should focus on optimizing the activation process and examining alternative activating agents. This might increase their applications in energy storage, water purification and electromagnetic wave absorption, leading to more effective and long-lasting solutions in these fields. Future research should investigate the scalability of manufacturing ACPs from various other agricultural waste products, which could result in more affordable and environmentally friendly waste recycling procedures.

Research Highlights

1. Preparation of Activated Carbon in Pellets form (ACPs) from date palm leaves by LiCl activation at 700 ℃ in a nitrogen environment, using a multi-step heating profiles.
2. Characterize of Young's modulus, crystalline structure, surface area and electrical conductivity of the ACPs produced as a function of LiCl concentrations by moles.

Acknowledgement

The authors extend their appreciation to the Deanship of Research and Graduate Studies at King Khalid University for funding this work through small-group research under grant number RGP 1/50/45.

Conflict of Interest

None.

References

1. Bhat, Md Yasir, Nitish Yadav and S. A. Hashmi. "Pinecone-derived porous activated carbon for high performance all-solid-state electrical double layer capacitors

fabricated with flexible gel polymer electrolytes." *Electrochim Acta* 304 (2019): 94-108.

2. Song, Xinyu, Xinlong Ma, Yun Li and Liang Ding, et al. "Tea waste derived microporous active carbon with enhanced double-layer supercapacitor behaviors." *Appl Surf Sci* 487 (2019): 189-197.
3. Herde, Zachary D., Ruchira Dharmasena, Gamini Sumanasekera and Jaya Shankar Tumuluru, et al. "Impact of hydrolysis on surface area and energy storage applications of activated carbons produced from corn fiber and soy hulls." *Carbon Resour Convers* 3 (2020): 19-28.
4. Yue, Jing, Jiaqi Yu, Shaohua Jiang and Yiming Chen. "Biomass carbon materials with porous array structures derived from soybean dregs for effective electromagnetic wave absorption." *Diam Relat Mater* 126 (2022): 109054.
5. Ratajczak, Paula, Matthew E. Suss, Friedrich Kaasik and François Béguin. "Carbon electrodes for capacitive technologies." *Energy Storage Mater* 16 (2019): 126-145.
6. Ndagijimana, Pamphile, Hongwei Rong, Pancras Ndokoye and Jean Pierre Mwizerwa, et al. "A review on activated carbon/graphene composite-based materials: Synthesis and applications." *J Clean Prod* 417 (2023): 138006.
7. Li, Xiaoyu, Dong Han, Mingyang Zhang and Bin Li, et al. "Removal of toxic dyes from aqueous solution using new activated carbon materials developed from oil sludge waste." *Colloids Surf A: Physicochem Eng Asp* 578 (2019): 123505.
8. Abd Rashid, Ramlah, Mohd Azlan Mohd Ishak and Kasim Mohammed Hello. "Adsorptive removal of methylene blue by commercial coconut shell activated carbon." *Sci Lett* 12 (2018): 77-101.
9. Qanytah, Q., Khaswar Syamsu, Farah Fahma and Gustan Pari. "Characterization of ball-milled bamboo-based activated carbon treated with $KMnO_4$ and KOH as activating agents." *Bioresour* 15 (2020): 8303.
10. Salomón, Yamil L. de O., Jordana Georgin, Dison SP Franco and Matias S. Netto, et al. "High-performance removal of 2, 4-dichlorophenoxyacetic acid herbicide in water using activated carbon derived from Queen palm fruit endocarp (*Syagrus romanzoffiana*)." *J Environ Chem Eng* 9 (2021): 104911.
11. Tobi, Ayinla Ridwan, J. O. Dennis, H. M. Zaid and A. A. Adekoya, et al. "Comparative analysis of physiochemical properties of physically activated carbon from palm bio-waste." *J Mater Res Technol* 8 (2019): 3688-3695.
12. Tran Thi Dieu, Huyen, Kanruethai Charoensook, Hung-Chun Tai and Yao-Tung Lin, et al."Preparation of activated carbon derived from oil palm empty fruit bunches and its modification by nitrogen doping for supercapacitors." *J Porous Mater* 28 (2021): 9-18.
13. Saleem, Junaid, Usman Bin Shahid, Mouhammad Hijab and Hamish Mackey, et al. "Production and applications of activated carbons as adsorbents from olive stones." *Biomass Convers Biorefin* 9 (2019): 775-802.
14. Sharma, Gaurav, Shweta Sharma, Amit Kumar and Chin Wei Lai, et al. "Activated carbon as superadsorbent and sustainable material for diverse applications." *Adsorp Sci Technol* (2022): 4184809.
15. Abdelrahman, Abubaker Elsheikh, Fatima Musbah Abbas and Abdul Kariem Arof. "Crystallite parameters, amorphous contents and surface functional groups, contents of activated carbon prepared from KOH treated pre-carbonized date palm leaves (*Phoenix dactylifera* L.)." (2023).
16. Zhou, Yibei, Juan Ren, Li Xia and Qiaoji Zheng, et al. "Waste soybean dreg-derived N/O co-doped hierarchical porous carbon for high performance supercapacitor." *Electrochim Acta* 284 (2018): 336-345.
17. Abbas, Fatima Musbah, Zehbah Ali Al Ahmad, Rehab Omer Elnour Elgezouly and Abubaker Elsheikh Abdelrahman. "Characterization of pores size, surface area and fractal di-mensions of activated carbon powder prepared from date palm leaves." (2022).
18. Ao, Wenya, Jie Fu, Xiao Mao and Qinhao Kang, et al. "Microwave assisted preparation of activated carbon from biomass: A review." *Renew Sustain Energy Rev* 92 (2018): 958-979.
19. Inal, I. Isil Gurten and Zeki Aktas. "Enhancing the performance of activated carbon based scalable supercapacitors by heat treatment." *Appl Surf Sci* 514 (2020): 145895.
20. Abbas, Fatima Musbah, Zehbah Ali Al Ahmad, Rehab Omer Elnour Elgezouly and Abubaker Elsheikh Abdelrahman. "Characterization of carbon pellets prepared from date palm leaves (*Phoenix dactylifera* L.) by compression pressure: X-ray diffraction measurements and applications." (2022).
21. Okman, Irem, Selhan Karagöz, Turgay Tay and Murat Erdem. "Activated carbons from grape seeds by chemical activation with potassium carbonate and potassium hydroxide." *Appl Surf Sci* 293 (2014): 138-142.
22. Hunsom, Mali and Chaowat Autthanit. "Adsorptive purification of crude glycerol by sewage sludge-derived activated carbon prepared by chemical activation with H_3PO_4, K_2CO_3 and KOH." *Chem Eng J* 229 (2013): 334-343.
23. Chowdhury, Shamik, Sharadwata Pan, Rajasekhar Balasubramanian and Papita Das. "Date palm based activated carbon for the efficient removal of organic dyes from aqueous environment." *Sustain Agric Rev 34: Date Palm for Food, Medicine and the Environment* (2019): 247-263.
24. Hussain, Ahmad, Aamir Farooq, Mohammad Ismail Bassyouni and Hani Hussain Sait, et al. "Pyrolysis of Saudi Arabian date palm waste: A viable option for converting waste into wealth." (2014).
25. Pagketanang, Thanchanok, Apichart Artnaseaw, Prasong Wongwicha and Mallika Thabuot. "Microporous activated carbon from KOH-activation of rubber seed-shells for application in capacitor electrode." *Energy Procedia* 79 (2015): 651-656.
26. Chanpee, Sirayu, Napat Kaewtrakulchai, Narathon Khemasiri and Apiluck Eiad-Ua, et al. "Nanoporous carbon from oil palm leaves *via* hydrothermal carbonization-combined KOH activation for paraquat removal." *Molecules* 27 (2022): 5309.
27. Yakout, S. M. and G. Sharaf El-Deen. "Characterization of activated carbon prepared by phosphoric acid activation of olive stones." *Arab J Chem* 9 (2016): S1155-S1162.
28. Wang, Jun-Feng, Christopher D. Bown, Biao Chen and L. Trevor Young. "Identification of mood stabilizer-regulated genes by differential-display PCR." *Int J Neuropsychopharmacol* 4 (2001): 65-74.
29. Won, Eunsoo and Yong-Ku Kim. "An oldie but goodie: Lithium in the treatment of bipolar disorder through neuroprotective and neurotrophic mechanisms." *Int J Mol Sci* 18 (2017): 2679.
30. Zhang, Jian, Lu He, Zhong Yang and Lihong Li, et al. "Lithium chloride promotes proliferation of neural stem cells *in vitro*, possibly by triggering the Wnt signaling pathway." *Anim Cells Syst* 23 (2019): 32-41.
31. Song, Ruiqi, Tonghua Zou, Jianbo Chen and Xiaobing Hou, et al. "Study on the physical properties of LiCl solution." *IOP Conf Ser Mater Sci Eng* (2019).
32. Abbas, Fatima Musbah, Abubaker Elsheikh Abdelrahman and Abdul Kariem Arof. "Specific surface area and spring lengths between two cubic volumes structure of the activated carbon pellets, from palm leaves, treated with KOH and carbonized at different temperature." (2023).
33. Reza, Md Sumon, Shammya Afroze, Kairat Kuterbekov and Asset Kabyshev, et al. "Advanced applications of carbonaceous materials in sustainable water treatment, energy storage and CO_2 capture: A comprehensive review." *Sustainability* 15 (2023): 8815.
34. Liu, Yuxuan, Xinhua Cheng and Shenghui Zhang. "Hierarchically porous carbon derived from tobacco waste by one-step molten salt carbonization for supercapacitor." *Carbon Letters* 32 (2022): 251-263.
35. Richards, B. P. "Relationships between interlayer spacing, stacking order and crystallinity in carbon materials." *J Appl Crystallogr* 1 (1968): 35-48.
36. Dresselhaus, M. S., A. W. P. Fung, A. M. Rao and S. L. Di Vittorio, et al. "New techniques for activated carbon fibers." *Carbon* 30 (1992): 1065-1073.
37. Arof, Abdul Kariem, M. Z. Kufian, M. F. Syukur and M. F. Aziz, et al. "Electrical double layer capacitor using poly (methyl methacrylate)–C_4BO_8Li gel polymer electrolyte and carbonaceous material from shells of mata kucing (*Dimocarpus longan*) fruit." *Electrochim Acta* 74 (2012): 39-45.
38. Azahar, A. A., M. D. Nurhafizah, N. Abdullah and A. Ul-Hamid. "A review on the palm oil waste thermal degradation analysis and its kinetic triplet study." *Bioenergy Res* 16 (2023): 1467-1492.
39. Faber, Kristin, Felix Badaczewski, Wilhelm Ruland and Bernd M. Smarsly. "Investigation of the microstructure of disordered, non-graphitic carbons by an advanced analysis method for wide-angle x-ray scattering." *Z fur Anorg Allg Chem* 640 (2014): 3107-3117.
40. Dolah, B. N. M., M. A. R. Othman, M. Deraman and N. H. Basri, et al. "Supercapacitor electrodes from activated carbon monoliths and carbon nanotubes." *J Phys Conf Ser* 431 (2013): 012015.

41. Yulianti, Riyani Tri, Fredina Destyorini, Yuyun Irmawati and Slamet Priyono, et al. "High capacitance performance of hierarchically SiO_2 self-doped porous activated carbon derived from palm empty fruit bunches." *J Energy Storage* 71 (2023): 108153.

42. Kacprzak, Andrzej and Renata Włodarczyk. "Utilization of organic waste in a direct carbon fuel cell for sustainable electricity generation." *Energies* 16 (2023): 7359.

How to cite this article: Fatima, Musbah Abbas, Ahlam Khalofa, Abdelrahman, Abubaker Elsheikh, and Selma Elsheikh Abdelrahman. "Activated Carbon (AC) Derived from Pre-carbonized Date Palm Leaves (PCDPLs) Activated with Lithium Chloride (LiCl): Physical and Electrical Properties." *Mol Biol* 14 (2025): 472.